(29) Bauer, B. J.; Hanley, B.; Muroga, Y. *Polym. Commun.* **1989**, *30*, 19.
(30) Roovers, J. E. L.; Bywater, S. *Macromolecules* **1972**, *5*, 385.
(31) Bauer, B. J.; Fetters. L. J. *Rubber Chem. Technol.* **1978**, *52*, 406.
(32) Glinka, C., private communication.
(33) Benoit, H. *J. Polym. Sci.* **1953**, *11*, 561.
(34) Burchard, W. *Macromolecules* **1977**, *10*, 919.
(35) Roovers, J.; Bywater, S. *Macromolecules* **1974**, *7*, 443.
(36) Roovers, J.; Toporowski, P. M. *J. Polym. Sci., Polym. Phys. Ed.* **1980**, *18*, 1907.
(37) Schmidt, M.; Burchard, W. *Macromolecules* **1981**, *14*, 210.
(38) Zimm, B. H.; Stockmayer, W. H. *J. Chem. Phys.* **1949**, *17*, 1301.
(39) Daoud, M.; Cotton, J. P. *J. Phys. (Les Ulis, Fr.)* **1982**, *43*, 531.
(40) Douglas, J. F.; Freed, K. F. *Macromolecules* **1984**, *17*, 2344.
(41) van Krevelen, D. W. *Properties of Polymers*: Elsevier: Amsterdam, 1976.
(42) Nishi, T.; Wang, T. T.; Kwei, T. K. *Macromolecules* **1975**, *8*, 227.
(43) Yang, H.; Hadziioannou, G.; Stein, R. S. *Sci. Phys. Ed.* **1983**, *21*, 159.
(44) Halary, J. L.; Ubrich, J. M.; Monnerie, L.; Yang, H.; Stein, R. S. *Polym. Commun.* **1985**, *26*, 73.
(45) de Gennes, P. G. *Scaling Concepts in Polymer Physics*; Cornell University Press: New York, 1979; Chapter IV.
(46) Owens, J. N.; Koberstein, J. T.; Gancarz, I.; Russell, T. P. *Macromolecules*, accepted for publication.
(47) Sanchez, I. C.; Lacombe, R. H. *J. Phys. Chem.* **1976**, *80*, 2352.
(48) Lacombe, R. H.; Sanchez, I. C. *J. Phys. Chem.* **1976**, *80*, 2568.
(49) Eichinger, B.; Flory, P. J. *Trans. Faraday Soc.* **1968**, *64*, 2038.
(50) Flory, P. J. *Discuss. Faraday Soc.* **1970**, *49*, 7.
(51) Brandrup, J., Immergut, E. H., Eds. *Polymer Handbook*; Wiley: New York, 1975.
(52) Hashimoto, T. *Current Topics in Polymer Science*; Ottenbrite, R. M., Utracki, L. A., Inoue, S., Eds.; Hanser Publishers: Munich, 1987; Vol. II, p 199.
(53) Stanley, H. E. *Introduction to Phase Transitions and Critical Phenomena*; Oxford University Press: New York, 1971.
(54) de Gennes, P. G. *J. Phys. (Les Ulis, Fr.)* **1977**, *38*, L-441.
(55) Gilmer, J. W.; Bringuier, A. G.; Sremcich, P. S. *Macromolecules*, submitted for publication.

Registry No. PVME, 9003-09-2; PS, 9003-53-6.

Tracer Diffusion of Linear Polystyrene in Entanglement Networks

Norio Nemoto,* Masahiro Kishine, Tadashi Inoue, and Kunihiro Osaki

Institute for Chemical Research, Kyoto University, Uji, Kyoto-fu 611, Japan.
Received March 29, 1989; Revised Manuscript Received June 26, 1989

ABSTRACT: The tracer diffusion coefficient D_{tr}^{∞} of linear polystyrenes (PS) with weight-average molecular weights M_w from 6100 to 2 890 000 was measured in entanglement networks of PS with M_ws much higher than the molecular weight of the respective diffusants at temperature of 30 °C by using forced Rayleigh scattering technique. Total polymer concentration C was 13 and 18 wt %, and C of the diffusant was fixed at 1 wt %. Dibutyl phthalate was used as solvent. D_{tr}^{∞} data at C = 13 and 18 wt % and also those obtained at 40.6 wt % in an earlier study were found to be superposed on one master curve by using two parameters, an effective friction coefficient of a segment ζ and the molecular weight between entanglements M_e, for reduction. Reduced D_{tr}^{∞} was proportional to M^{-1} and $M^{-2.5}$ in the unentangled ($M/M_D < 1$) and the entangled region ($M/M_D > 1$), respectively, where M_D is the molecular weight at the intersection point and is very close to M_e.

Introduction

In a previous study,[1] the tracer diffusion coefficient D_{tr} of linear polystyrenes (PS) with molecular weights M_N was measured in entanglement networks of matrix PS with molecular weights M_P in the concentrated regime by using the forced Rayleigh scattering technique. We found that D_{tr} asymptotically took a value of D_{tr}^{∞} independent of the molecular weight M_P of PS matrix with $M_P > 5M_N$, and also that D_{tr}^{∞} obtained exhibited a break at a characteristic molecular weight M_D, which was very close to the molecular weight between entanglements M_e of the network. D_{tr}^{∞} was inversely proportional to M_N below M_D, which indicates that the diffusing chain can be pictured as a free-draining Rouse chain with an effective segment friction coefficient of $\zeta(C,T)$. Above M_D, the dependence of D_{tr}^{∞} on M_N was expressed by the power law $D_{tr}^{\infty} \propto M_N^{-\alpha}$ with the exponent α = 2.5 for the largest value of M_N/M_e = 30 studied. This behavior is in contrast to the tracer diffusion behavior in melts[6] where α is very close to 2, in agreement with the prediction of the reptation theory.[17] A similar difference in the exponent α between concentrated solutions and melts was also observed for self-diffusion behavior.[1,2-9] Thus the retardation effect on diffusion due to the elastic entanglement network characterized by M_e appeared stronger in the concentrated regime than in melts.

In the semidilute regime, there are large amounts of self-diffusion and tracer diffusion data.[23-31] Among them, the most extensive study on D_{tr}^{∞} behavior made by Yu and co-workers[10] showed that D_{tr}^{∞} exhibited quite strong molecular weight dependence, such that α may be close to 3. Then acceptance of all values of the exponents reported leads to supposition that the exponent tends to monotonically decrease with increasing concentration from a value of 3 in the semidilute regime to 2 in melts. However, we may point out that exponents for concentrated solution and melt data were obtained in the highly entangled region of $M_N/M_e > 10$, whereas a maximum value of M_N/M_e attained is less than 10 for semidilute solution data. Therefore there remains an ambiguity with respect to the exponent 3, which is only apparent and decreases with increasing M_N/M_e toward a somewhat lower value at large M/M_e values as is observed for melt data. It should be also noted that the exponent α for the self-diffusion coefficient D_s in the semidilute regime is not in complete agreement with the theoretical value of 2 but appears to be near 2.

The present investigation is first aimed at extending D_{tr}^{∞} measurements in the semidilute regime to the region

0024-9297/90/2223-0659$02.50/0

Table I
Characteristics of Polystyrene

sample code	$M_w/10^4$	M_w/M_n	sample code	$M_w/10^4$	M_w/M_n
A5000[a]	0.61	1.04	F40[a]	35.5	1.02
F1[a]	1.03	1.02	F80[a]	77.5	1.01
F2[a]	1.67	1.02	F128[a]	126	1.05
F4[a]	4.39	1.01	F288[a]	289	1.09
F10[a]	10.2	1.02	F550[b]	548	1.15
F20[a]	18.6	1.07	F850[b]	842	1.17

[a] Labeled with a photobleachable dye. [b] Used as matrix polymer.

of $M_N/M_e > 10$ in order to erase the above-mentioned ambiguity. Results on dibutyl phthalate solutions of PS at concentrations of 13 and 18 wt %, which is the same polymer–solvent pair tested in the earlier study, show that the dependence of D_{tr}^{∞} on M_N can be expressed by two straight lines with slopes of −1 and −2.5 below and above M_D, respectively, where M_D is close to M_e at respective concentrations. All data in the semidilute and the concentrated regime were reduced, which is the second purpose of the present study, following a two-parameter scheme that has been shown to be quite useful for analysis of viscoelastic data.[11-13] Here the two parameters are ζ and M/M_e. We found that one master curve can be obtained by superposition of reduced D_{tr}^{∞} data.

Experimental Section

Materials. Twelve samples of narrow-distribution polystyrenes (PS, Toyo Soda) with different molecular weights were used in this study. Their sample codes, weight-average molecular weights M_w, and ratios M_w/M_n are listed in Table I. Ten PS samples except the two highest molecular weight PSs that were used as a matrix polymer were labeled with a photobleachable dye of 2-nitro-4-carboxy-4′-(dimethylamino)stilbene following the labeling procedure described in earlier papers.[14,15] GPC combined with low-angle light scattering measurements showed that there was no change in either the molecular weight or the molecular weight distribution of the polymers during the labeling procedure. Distilled dibutyl phthalate (DBP), a good solvent for PS, was used.

Test solutions with PS molecular weights less than that of the sample F550 used as the matrix polymer were prepared by dissolving a weighed amount of dust-free labeled PS, unlabeled PS, and DBP in an excess amount of methylene dichloride, stirring for a couple of days to complete homogeneous mixing, and subsequently evaporating methylene dichloride very slowly from the solutions. Solutions containing higher molecular weight PS samples were prepared by applying a freeze-drying procedure on molecularly mixed benzene solutions of a weighed amount of polymers and the solvent for a week. Polymer concentration was determined by assuming that very slight decrease in total weight of the PS–DBP solutions during the freeze-drying procedure was due to evaporation of DBP. Two series of PS-DBP solutions with total polymer concentration C of 13 and 18 wt % were prepared. The concentration of the labeled PS component was fixed at 1 wt % irrespective of molecular weight of the sample.

Method. Forced Rayleigh scattering measurements were performed with an instrument described elsewhere.[15] Monochromatic light of an Ar ion laser (λ = 488 nm) and of a He–Ne laser (λ = 633 nm) were used as a writing and reading beam, respectively. Acquisition and analysis of light intensity data $I_d(t)$ diffracted from the solution were handled with a homemade processor. Measurements were made at 30 ± 0.05 °C on all solutions.

Results

1. Data Analysis. Time profiles of $I_d(t)$ diffracted at respective Bragg angles from the solutions were fitted

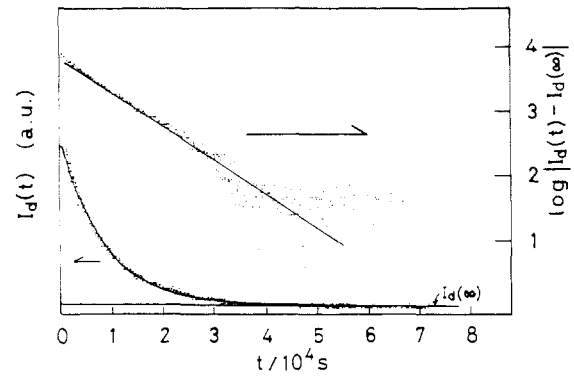

Figure 1. Time profile of $I_d(t)$ diffracted from the solution of F288 in F850–DBP with C = 18 wt % at T = 30 °C. Grating spacing is 2 μm. The solid curve is the curve fitted to data from the 30th to the 600th point with eq 1. The plot of log $|I_d(t) - I_d(\infty)|$ against t is represented by a straight line over a large time interval, which indicates the applicability of eq 1 with the contrast A/B_1. The value of $I_d(\infty)$ indicated in the figure is 260 count/s.

by eq 1 with a single decay rate Γ_d to all PS samples.

$$I_d(t) = \{A \exp(-\Gamma_d t) + B_1\}^2 + B_2^2 \quad (1)$$

Here A is amplitude and B_1 and B_2 are contributions from coherent and incoherent background optical fields, respectively. An example is shown in Figure 1 for the highest molecular weight PS sample F288 in 18 wt % F850–DBP solutions at grating spacing d = 2 μm. The fitted curve, given by the solid curve in the figure, accurately reproduces the time dependence of $I_d(t)$ and gives $\Gamma_d = 5.86 \times 10^{-5}$ s^{-1}, from which D_{tr} is estimated as 5.94×10^{-14} cm^2/s by the use of $\Gamma_d = D_{tr}q^2$. Here q is the wave vector to be calculated from $q = 2\pi/d$. In the figure, we also show a plot of log $|I_d(t) - I_d(\infty)|$ against t where $I_d(\infty)$ is a value of $I_d(t)$ observed at the longest time end, that is, the base-line value. Very good linearity of the plot over a large time interval indicates that contrast in A/B_1 is quite high and the measurement was pertinently excuted with our homemade FRS instrument. It may be noted that correction of intensity fluctuations of the reading laser beam considerably improves data fitting in cases where the measurement time exceeded 1 day.

Although eq 1 was sufficient for analysis of most data obtained (the variance is less than 0.08), we found deviations from single exponential of the decay function in some data. The cumulant fit to the second order gave a variance of about 0.3 and a 30–40% higher D_{tr} value than that obtained by the forced fit with eq 1. The deviations seem to have occurred irrespective of the PS molecular weight tested. For data fitting in these case, we usually used a modification of eq 1, which allowed a deviation of the base line from the measured value and estimated Γ_d. For each solution, FRS measurements were performed at at least two different d values and if estimated Γ_d/q^2 values agreed with each other to an accuracy of 10%, we took their average as a D_{tr} value. Otherwise, we estimated D_{tr} from the slope of a plot of Γ_d against q^2. Examples of such a plot for a D_{tr} value larger than 10^{-12} cm^2/s are given elsewhere.[14,22] Figure 2 gives plots of Γ_d against q^2 for three PS solutions that gave D_{tr} values less than 10^{-12} cm^2/s. From the good proportionality of Γ_d to q^2, we could estimate D_{tr} values to an accuracy of about 10%, even in the range $D_{tr} < 10^{-12}$ cm^2/s.

2. Molecular Weight and Concentration Dependences of D_{tr}. It has been shown by two research

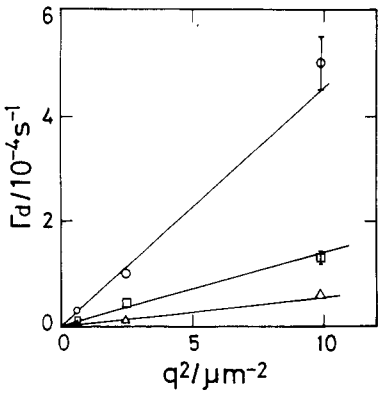

Figure 2. Decay rate Γ_d is plotted against the square of the wave vector q for three PS–DBP solutions. From the top, F128 in F850 at C = 18 wt %, F288 in F850 at C = 13 wt %, and F288 in F850 at C = 18 wt %. Bars to respective data points indicate an experimental error of 10% expected in the measurements. The tracer diffusion coefficient D_{tr} is estimated from the slope of the plot as 4.8×10^{-13}, 1.6×10^{-13}, and 4.3×10^{-14} cm^2/s for the respective solutions.

groups[7,16] and confirmed by us[1] that the tracer diffusion coefficient D_{tr} becomes independent of the molecular weight of a matrix polymer when a ratio M_P/M_N exceeds about 5.[7,16] Therefore we measured D_{tr} of PS samples from A5000 to F128 in one entangled solution with $M_P > 7M_N$ and assigned a measured D_{tr} value as D_{tr}^{∞}, which may be obtained in an entanglement network with infinite molecular weight. For the highest molecular weight sample F288, on the other hand, the measurement was conducted in a solution of sample F850, whose molecular weight is about three times larger than that of F288, thus D_{tr} obtained may not be assigned as D_{tr}^{∞} at once. The previous study[1] on the self-diffusion coefficient D_s of concentrated PS solutions showed that D_s asymptotically approached D_{tr}^{∞} with increasing M for $M/M_e > 10$. Since M_N/M_e is larger than 10 for this sample as will be shown later, it seems reasonable to assume that the measured value of D_{tr} may be very close to D_{tr}^{∞}. Hereafter the symbol M will be used as the molecular weight of a probe chain by abbreviating the suffix N.

In Figure 3, D_{tr}^{∞} of two series of solutions with C = 13 and 18 wt % is plotted against M on a double-logarithmic scale. Table II lists values of D_{tr}^{∞} at T = 30 °C. As a measure of the strength of entanglement coupling, the position of M_e on the abscissa is indicated by arrows to each concentration in the figure. Here we estimated M_e employing the empirical equation[19]

$$M_e = 1.8 \times 10^4 C^{-1} \text{ (g/cm}^3\text{)}^{-1} \quad (2)$$

M_e values are calculated as 130 000 and 96 000 at C = 13 and 18 wt %, respectively. Equation 2 was obtained from the rubbery plateau modulus G_N of PS–Aroclor solutions by use of the relation $G_N = CRT/M_e$.[12] Dibutyl phthalate used as a solvent for D_{tr}^{∞} measurements is different from Aroclor for viscoelastic measurements. It is uncertain whether both solvents are good for PS to the same extent. Therefore viscoelastic measurements on the PS–DBP system might give an M_e versus C relation slightly different from eq 2. However, later analysis by using eq 2 shows that the equation is useful for an estimate of M_e of the DBP solutions of PS at C = 13 and 18 wt %. In the figure, concentrated solution data at C = 40.6 wt % and T_r = 60 °C obtained in the previous study[1] are also given for comparison. The figure clearly shows that D_{tr}^{∞} behavior in the semidilute regime is quite similar to that in the concentrated regime. The molecular weight

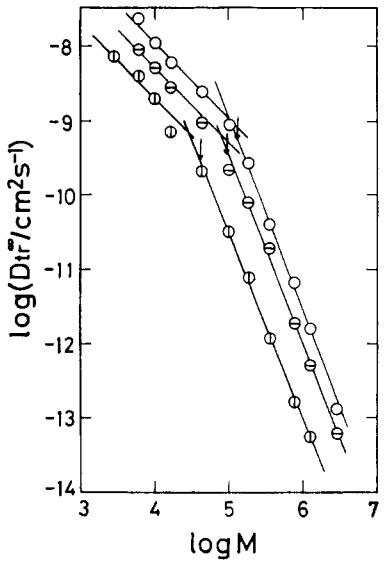

Figure 3. Tracer diffusion coefficient D_{tr}^{∞} of two series of PS–DBP solutions with C = 13 and 18 wt % is plotted against the molecular weight M of the diffusant. Concentrated solution data at C = 40.6 wt % and T_r = 60 °C obtained in the earlier study[1] are also given for comparison. Symbols: (○) 13, (⊖) 18, and (⊙) 40.6 wt %. An arrow indicates the value of M_e at each concentration calculated from eq 2. Two straight lines with slopes of −1 and −2.5 drawn empirically for the data at each concentration are going to be used for later discussion.

Table II
Values of the Tracer Diffusion Coefficient D_{tr} in PS–DBP Solutions at T = 30 °C

$D_{tr}^{\infty}/10^{-11}$ cm^2 s^{-1}			$D_{tr}^{\infty}/10^{-11}$ cm^2 s^{-1}		
	C, wt %			C, wt %	
sample	13	18	sample	13	18
A5000 in F80	2300	900	F20 in F288	27	8.0
F1 in F80	1100	510	F40 in F550	4.0	1.9
F2 in F80	600	290	F80 in F850	0.66	0.19
F4 in F80	250	96	F128 in F850	0.16	0.045
F10 in F128	90	22	F288 in F850	0.014	0.0055

dependence varies at around M_e from $D_{tr}^{\infty} \propto M^{-1-1.2}$ to $D_{tr}^{\infty} \propto M^{-2.5}$ in the highly entangled region. Thus we may conclude that the exponent 2.5 holds over a fairly wide range of concentration for well-entangled systems. This is in contrast to the relation $D_{tr}^{\infty} \propto M^{-2}$ either predicted by the reptation theory[17] or observed for PS melts.

3. Data Reduction. There seems to be consensus that linear viscoelastic properties of entangled polymers in solution as well as in melt can be systematically described in terms of the two parameters, $\zeta(C,T)$ and $M_e(C)$.[11] The two-parameter scheme has been shown to be also applicable for nonlinear viscoelasticity of entangled polymer solutions.[13] Then we expect that diffusion of polymer chains through entanglement networks may be also characterized by the same two parameters. Applicability of the concept has been already pursued for self-diffusion of polymers by expressing D_s as a product of two separate contributions $f_2(\zeta)$ and $g_2(C,M)$:

$$D_s = f_2(\zeta) g_2(C,M) \quad (3)$$

Here f_2 represents a contribution from micro-Brownian motion of a segment and is proportional to T/ζ. The g_2 represents the effect of the topological interaction with surrounding polymer chains.

Concerning tracer diffusion, data analysis proceeded as follows. Under the experimental condition that the molecular weight of the matrix polymer was made suffi-

ciently higher than that of the diffusant, the matrix chains are supposed to be immobile during the characteristic diffusion time of the probe chain, so that they respond as an elastic network characteristic of the mesh size corresponding to M_e. Then, the retardation effect on tracer diffusion of a probe chain due to the entangled matrix may be assumed to be expressible in terms of a function of the ratio M/M_e. On the other hand, local segmental motions are independent of M at high M_P but depend on C in a very complicated fashion.[18] In the semidilute regime, solvent viscosity and screened hydrodynamic interaction determine the magnitude and C dependence of ζ,[19] while chain packing or the free volume plays an essential role in the concentrated regime.[11] In a previous sedimentation study of poly(methyl methacrylate) in semidilute solutions of PS in thiophenol,[20] we showed that if the coil size of the diffusant is sufficiently smaller than the mesh size of the network, the diffusant may be free from the effect of topological interaction with surrounding chains and may behave as a free-draining Rouse chain with an effective segment friction coefficient ζ in which the effect of the screened hydrodynamic interaction is absorbed. Since the same ζ value can be used as the effective friction coefficient of a segment in any high molecular weight chain at constant C and T, a probe chain may be substituted for the free-draining Rouse chain if there were no topological interaction with surrounding matrix chains. By expressing the entanglement effect from the elastic network as a function $\psi^{-1}(M/M_e)$, which was introduced in the previous study,[20] we rewrite eq 3 for $D_{tr}^{\infty}(M)$ as

$$D_{tr}^{\infty}(M) = \frac{KT}{\zeta M}\psi^{-1}(M/M_e) \quad (4)$$

where K is a constant independent of M, C, and T. Equation 4 means that the friction coefficient, f, of a whole chain is given by $f = n\zeta\psi$ where n is the number of segments per chain. As was presumed in the previous paragraph, ψ^{-1} may be set equal to unity for a chain with $M \ll M_e$. For example, $D_{tr}^{\infty}(0.1M_e)$ at $M = 0.1M_e$ may be written to very good approximation as

$$D_{tr}^{\infty}(0.1M_e) = KT/0.1\zeta M_e \quad (5)$$

From eq 4 and 5, we see that a reduced variable $D_{tr}^{\infty}(M)/D_{tr}^{\infty}(0.1M_e)$ is a function of only M/M_e:

$$D_{tr}^{\infty}(M)/D_{tr}^{\infty}(0.1M_e) = 0.1(M/M_e)^{-1}\psi^{-1}(M/M_e) \quad (6)$$

A value of $D_{tr}^{\infty}(0.1M_e)$ at each concentration is easily read from interpolation of respective data in Figure 3 by using an M_e value calculated from eq 2. Figure 4 shows results of the superposition of three sets of $D_{tr}^{\infty}(M)/D_{tr}^{\infty}(0.1M_e)$ versus M/M_e plots at C = 13, 18, and 40.6 wt %. It is evident that superposition has been successfully achieved within a deviation of about 30%. It should be emphasized that within a framework of the two-parameter scheme, one master curve has been obtained for tracer diffusion data in the semidilute and the concentrated regime without any adjustable parameter. The master curve can be represented to very good approximation by two straight lines intersecting at $M/M_e \simeq 1$. The slope of unity for $M/M_e < 1$ proves that the free-draining chain model is applicable for tracer diffusion through the network in this low molecular weight range. For $M/M_e > 1$, the slope of −2.5 appears to persist up to the largest M/M_e value of 30 studied. D_{tr}^{∞} of PS melts is found to become asymptotically proportional to M^{-2} for $M/M_e > 3$. At present, we do not regard the large exponent 2.5 for solutions as the apparent or transient value in the intermediate region between the unentangled and the highly entangled region. Then, the difference in the exponent α for $M/M_e > 10$ between solutions and melts is not in harmony with a view that the entanglement effect on diffusion can be expressed by one universal function of M/M_e for both of solutions and melts, which seems to hold for viscoelastic data.

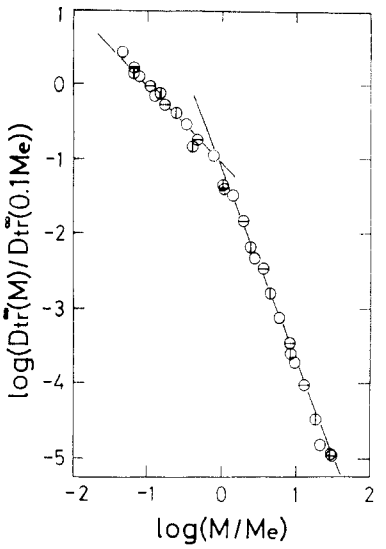

Figure 4. Reduced tracer diffusion coefficient $D_{tr}^{\infty}(M)/D_{tr}^{\infty}(0.1M_e)$ is plotted against the number of entanglements per chain M/M_e. The master curve can be represented to very good approximation by two straight lines with a slope of −1 for $M < M_e$ and of −2.5 for $M > M_e$. Symbols are the same as in Figure 3.

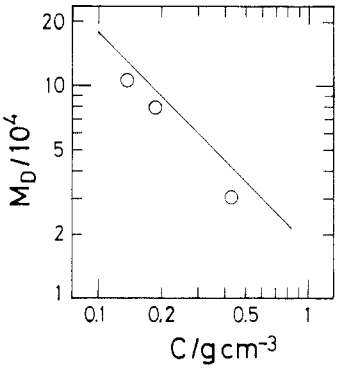

Figure 5. D_{tr}^{∞} data in Figure 3 is approximated by two straight lines with slopes of 1 and −2.5 in the low- and high-M region, respectively, and the molecular weight M_D estimated as the molecular weight at the intersecting point is plotted against C. The solid line is that given by eq 2.

The molecular weight at which the two straight lines intersect looks a little different from M_e. In order to examine this, the D_{tr}^{∞} curve at each concentration in Figure 3 was approximately expressed by two straight lines with the slopes of −1 and −2.5 in the low and the high M region, respectively, as is shown in Figure 3, and the molecular weight M_D was estimated as the molecular weight at each intersecting point. Results are shown on a double-logarithmic scale in Figure 5 where eq 2 is given as a solid line for comparison. M_D is only a little bit smaller than M_e (maximum 35%) and has slightly stronger concentration dependence ($\propto C^{-1.1}$) compared with M_e. If we take into account that M_D and M_e were estimated with quite different experimental techniques and methods, it would be better to say that agreement is not unsatisfactory. More diffusion measurements at different concentrations seem necessary for us to get a definite answer. Stated in another

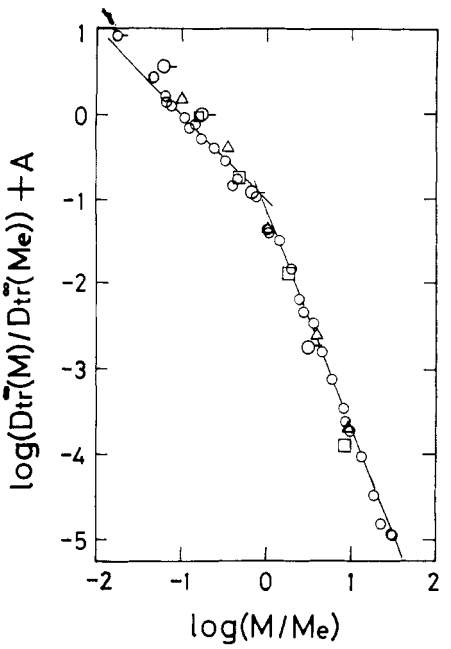

Figure 6. Reduced D_{tr}^{∞} data, $D_{tr}^{\infty}(M)/D_{tr}^{\infty}(M_e)$, of the PS–toluene system reported by Yu et al.[10] is superposed on the master curve of Figure 4 by vertically shifting the former data with the shift factor $A = -1.35$. Symbols for the PS–toluene data: (○) 5, (□) 10, and (△) 20 wt %. Unfilled circles are the data of the PS–DBP system given in Figure 4.

way, the fact of $M_D \simeq M_e$ made it possible to construct the master curve in Figure 4 by using M_e values determined from viscoelastic measurements. Finally it may be noted that use of $D_{tr}^{\infty}(M_D)$ at the interesting point is also successful for reduction and superposition of $D_{tr}^{\infty}(M)$. We preferred to use M_e and $D_{tr}^{\infty}(0.1M_e)$ for showing how viscoelastic and diffusion properties are consistent with each other in the concentration range investigated.

Discussion

In the Introduction, we referred to the work of Yu and co-workers,[10] in which D_{tr}^{∞} of PS in semidilute toluene solutions has a little stronger molecular weight dependence, i.e., the exponent being close to 3 in the range $1 < M/M_e < 10$. Since the exponent is different from our result of 2.5, we would like to analyze their data on the basis of the two-parameter scheme for comparison with the reduced data in Figure 4. For this purpose, their $D_{tr}^{\infty}(M)$ data at three concentrations of 5, 10, and 20 wt % were reduced by respective values of D_{tr}^{∞} at $M = M_e$ instead of $D_{tr}^{\infty}(0.1M_e)$, simply because $D_{tr}^{\infty}(0.1M_e)$ at $C = 20$ wt % could not be read from the corresponding curve in Figure 6 in ref 10. $D_{tr}^{\infty}(M_e)$ is of course influenced by the topological interaction with matrix chains. Strictly speaking, therefore, reduction in terms of $D_{tr}^{\infty}(M_e)$ is allowed only if entanglements affect $D_{tr}^{\infty}(M_e)$ by the same factor at every concentration. We found that their data at different concentrations can be fairly well superposed onto one another on one master curve. The reduced $D_{tr}^{\infty}(M)/D_{tr}^{\infty}(M_e)$ versus M/M_e curve of the PS–toluene system was then superposed on the master curve of the PS–DBP system in Figure 4 by shifting the former curve along the ordinate axis so that the both curves may agree at $M/M_e = 1$. As Figure 6 shows, agreement appears gratifying. Thus we may conclude that the two-parameter scheme is successful in describing the molecular weight and the concentration dependences of the tracer diffusion coefficient of a polymer chain through the entanglement network from the semidilute to the concentrated regime and that the exponent 2.5 in Figure 6 is a value commonly observed for D_{tr}^{∞} of entangled PS chains at finite concentration. This statement is expressed in terms of eq 3 by replacing D_s by D_{tr}^{∞}, as follows:

$$D_{tr}^{\infty}(M) = f_2'(C,T)g_2'(C,M) \tag{7}$$

$$f_2'(C,T) = K_2T/\zeta(C,T) \tag{8}$$

$$g_2'(C,M) = M^{-1} \quad M \lesssim M_D \simeq M_e$$
$$= M^{-1}(CM)^{-1.5} \quad M > M_D \simeq M_e \tag{9}$$

Here we used eq 2 for C dependence of M_e, and the constant K_2 along with ζ is not yet specified for the respective polymer–solvent system. Equations 7–9 may be examined at higher concentrations for the same PS-DBP system and also for entangled systems of different polymer species.

Finally we remark on the scaling theory,[19] which is frequently used for discussing static as well as dynamic properties of polymers in the semidilute regime. The most important quantity in the theory is the static (or dynamic) correlation length ξ_s (or ξ_H), which is related to the blob size (or the hydrodynamic radius) by a simple argument. Both ξ and M_e are independent of molecular weight above the overlapping threshold concentration C^* and have a similar concentration dependence above C^* in good solvent. Therefore they have been often treated as the same quantity or as at least as being proportional to each other. However, this idea is completely wrong. The ξ measurable by scattering methods (light, X-ray, neutron) is determined by the osmotic force, i.e., by the volume force, whereas M_e related to the entanglement phenomena is measurable only when the shear or tensile force is applied to sufficiently long polymer chains. For example, we can determine ξ of solutions of polymers with M less than M_e for $C > C^*$ but cannot evaluate M_e since the solutions are never entangled. Moreover, we showed in a previous paper[21] that the characteristic distance between entanglement loci, ξ_e, calculated from M_e is several times larger than the hydrodynamic correlation length ξ_H. If the size of the blob is represented by ξ_H and ideal chain statistics is applied, a large number of connected blobs are contained in the distance ξ_e. In entanglement dynamics, then, each blob can be regarded as a segment with an effective friction coefficient into which effects of the screened hydrodynamic interaction and of the excluded volume are absorbed. It seems that the scaling theory developed so far is useful for treatment of static properties as well as local chain motions but not for the entanglement effect.

Acknowledgment. We are greatly indebted to Toyo Soda Co. Ltd. for supplies of PS samples. This study was partly supported by a Grant-in-Aid for Scientific Research (No. 62660653, No. 63470091) of the Ministry of Culture, Science and Education of Japan.

Registry No. PS, 9003-53-6; 2-nitro-4-carboxy-4′-(dimethylamino)stilbene, 65199-97-5.

References and Notes

(1) Nemoto, N.; Kojima, T.; Inoue, T.; Kishine, M.; Hirayama, T.; Kurata, M. *Macromolecules* **1989**, *22*, 3793.
(2) (a) Klein, J. *Nature (London)* **1978**, *271*, 143. (b) Klein, J.; Briscoe, B. J. *Proc. R Soc. London, Ser. A* **1979**, *365*, 53.
(3) Bartles, C. R.; Christ, B.; Graessley, W. W. *Macromolecules* **1984**, *17*, 2702.

(4) (a) Antonietti, M.; Coutandin, J.; Grütter, R.; Sillescu, H. *Macromolecules* **1984**, *17*, 798. (b) Antonietti, M.; Coutandin, J.; Sillescu, H. *Macromolecules* **1986**, *19*, 793.
(5) (a) Smith, B. A. *Macromolecules* **1982**, *15*, 469. (b) Smith, B. A.; Samulski, E. T.; Yu, L.-P.; Winnik, M. A. *Macromolecules* **1985**, *18*, 1901. (c) Smith, B. A.; Mumby, S. J.; Samulski, E. T.; Yu, L.-P. *Macromolecules* **1986**, *19*, 470.
(6) (a) Green, P. F.; Mills, P. J.; Palmstrom, C. J.; Mayer, J. W.; Kramer, E. J. *Phys. Rev. Lett.* **1984**, *57*, 2145. (b) Green, P. F.; Kramer, E. J. *Macromolecules* **1986**, *19*, 1108.
(7) Fleisher, G. *Polym. Bull.* **1984**, *11*, 75.
(8) Pearson, D. S.; Verstrate, G.; von Meerwall, E. D.; Schilling, F. G. *Macromolecules* **1987**, *20*, 1133.
(9) Watanabe, H.; Kotaka, T. *Macromolecules* **1987**, *20*, 530.
(10) Kim, H.; Chang, T.; Yohanan, J. M.; Wang, L.; Yu, H. *Macromolecules* **1986**, *19*, 2737.
(11) Ferry, J. D. *Viscoelastic Properties of Polymers*, 3rd ed.; John, Wiley: New York, 1980.
(12) Osaki, K.; Nishimura, Y.; Kurata, M. *Macromolecules* **1985**, *18*, 1153.
(13) Osaki, K.; Takatori, E.; Tsunashima, Y.; Kurata, M. *Macromolecules* **1987**, *20*, 525.
(14) Inoue, T.; Nemoto, N.; Kojima, T.; Kurata, M. *J. Soc. Rheol. Jpn.* **1988**, *16*, 72 (in Japanese); *Polym. J.* **1988**, *20*, 869.
(15) Inoue, T. Ph.D. Thesis, Kyoto University, 1988 (in Japanese).
(16) Deschamps, H.; Leger, L. *Macromolecules* **1986**, *19*, 2760.
(17) Doi, M.; Edwards, S. F. *J. Chem. Soc., Faraday Trans. 2* **1978**,*74*, 1789.
(18) In tracer diffusion, an extra degree of freedom associated with chain ends, is considered as an intrinsic property of the probe chain.
(19) de Gennes, P.-G. *Scaling Concepts in Polymer Physics*; Cornell University Press: Ithaca, NY, 1979.
(20) Nemoto, N.; Okada, S.; Inoue, T.; Kurata, M. *Macromolecules* **1988**, *21*, 1502.
(21) Nemoto, N.; Makita, Y.; Tsunashima, Y.; Kurata, M. *Macromolecules* **1984**, *17*, 2629.
(22) Nemoto, N.; Kojima, T.; Inoue, T.; Kurata, M. *Polym. J.* **1988**, *20*, 875.
(23) Callaghan, P. T.; Pinder, D. N. *Macromolecules* **1984**, *17*, 431.
(24) Marmonier, M. F.; Leger, L. *Phys. Rev. Lett.* **1985**, *55*, 1078.
(25) von Meerwall, E. D.; Amis, E. J.; Ferry, J. D. *Macromolecules* **1985**, *18*, 260.
(26) Numasawa, N.; Kuwamoto, K.; Nose, T. *Macromolecules* **1986**, *19*, 2593.
(27) Nemoto, N.; Landry, M. R.; Noh, I.; Kitano, T.; Wesson, J. A.; Yu, H. *Macromolecules* **1985**, *18*, 308.
(28) Wesson, J. A.; Noh, I.; Kitano, T.; Yu, H. *Macromolecules* **1984**, *17*, 431.
(29) Wheeler, L. M.; Lodge, T. P.; Hanleg, B.; Tirrell, M. *Macromolecules* **1987**, *20*, 1120.
(30) Philles, G. D. *Macromolecules* **1988**, *21*, 3101.
(31) Wheeler, L. M.; Lodge, T. P. *Macromolecules* **1989**, *22*, 2379.

Molecular Dynamics Simulation of the Condis State of Polyethylene†

D. W. Noid,* B. G. Sumpter,* and B. Wunderlich*

Chemistry Division, Oak Ridge National Laboratory, Oak Ridge, Tennessee 37831-6182, and Department of Chemistry, The University of Tennessee, Knoxville, Tennessee 37996-1600.
Received April 7, 1989; Revised Manuscript Received June 6, 1989

ABSTRACT: Using a realistic model for polyethylene (PE), the molecular dynamics technique is used to simulate atomic motion in a crystal. The calculations reveal conformational disorder above a critical temperature. The customarily assumed rotational isomers model is found to be a poor description of the crystal at elevated temperature. The rate of isomerization computed from molecular dynamics is compared to transition-state theory and leads to an activation energy of 23 kJ/mol, 6.3 kJ/mol above the single-bond rotation value. Classical heat capacities have been calculated and result in negative and positive deviations from $3R$, as was also observed experimentally. The negative expansion coefficient of the fiber axis is in good agreement with the experiment. A movie of the dynamics of the polyethylene crystal has been produced.

I. Introduction

In the study of crystals of flexible macromolecules, it has been demonstrated that a distinctly different type of mesophase with dynamic, conformational disorder can exist, the condis crystal.[1,2] Important ramifications of this conformational flexibility of PE chains on physical properties should include mechanical and dielectric relaxation, transport properties, and spectroscopy. Conformational disorder in isolated chains has been studied for many years using the Monte Carlo methods with the rotational isomeric model[3-5] in which the torsional angle, τ, is allowed to have only discrete values of 0 or $\pm 120°$. Recently, Yamamoto has used a continuous rotational model to study chain conformations in a crystal mean field.[6] One of the conclusions was that the rotational isomer model is not valid in a crystal environment. Several other studies have been made using molecular mechanics to understand the energetics of conformational disorder[7] and using normal mode theory[8] to clarify the effect of various conformational defects on infrared transitions.[9] Because these types of distortions or defects involve large-amplitude motion, which is anharmonic, it is not clear why the harmonic approximation (normal-coordinate analysis) would be valid and provide reliable results.

The purpose of this paper is to recognize the fact that conformational disorder in a polymer environment is a dynamic process and involves anharmonic motion. For this reason, we have used the molecular dynamics method (MD) to simulate conformational disorder more realisti-

† Research sponsored by the Division of Materials Sciences, Office of Basic Energy Sciences, U.S. Department of Energy, under Contract DE-AC05-840R21400 with Martin Marietta Energy Systems, Inc., and the National Science Foundation, Polymers Program, Grant No. 8818412.

0024-9297/90/2223-0664$02.50/0